Vapor−Liquid Coexistence Curves in the Critical Region and the Critical Temperatures and Densities of 1,1,1,2-Tetrafluoroethane (R-134a), 1,1,1-Trifluoroethane (R-143a), and 1,1,1,2,3,3-Hexafluoropropane (R-236ea)

Hirokazu Aoyama, Go Kishizawa, Haruki Sato,* and Koichi Watanabe

Department of Mechanical Engineering, Faculty of Science and Technology, Keio University, 3-14-1, Hiyoshi, Kohoku-ku, Yokohama 223, Japan

The vapor−liquid coexistence curves in the critical region of 1,1,1,2-tetrafluoroethane (R-134a), 1,1,1-trifluoroethane (R-143a), and 1,1,1,2,3,3-hexafluoropropane (R-236ea) were measured by a visual observation of the meniscus disappearance in an optical cell. Seventeen saturated-vapor and -liquid densities have been measured for R-134a. Thirty-five saturated-vapor and -liquid densities have been measured for R-143a. Twenty-seven saturated-vapor and -liquid densities have been measured for R-236ea. The level and location of the meniscus, as well as the intensity of the critical opalescence were considered in the determination of the critical temperature and density for each fluid. R-134a was found to have (374.083 ± 0.010) K and (509 ± 1) kg/m^3, R-143a, (345.860 ± 0.010) K and (434 ± 1) kg/m^3, and R-236ea, (412.375 ± 0.015) K and (568 ± 1) kg/m^3.

Introduction

We have already reported vapor-liquid coexistence curves and critical temperatures and densities of several CFC-alternative refrigerants: 1,1-difluoroethane (R-152a) (Higashi et al., 1987), 1,1,1,2-tetrafluoroethane (R-134a) (Kabata et al., 1989), 1,1-dichloro-2,2,2-trifluoroethane (R-123) (Tanikawa et al., 1991), 1-chloro-1,1-difluoroethane (R-142b) (Tanikawa et al., 1992), 1,1,2,2-tetrafluoroethane (R-134) (Tatoh et al., 1993), difluoromethane (R-32), pentafluoroethane (R-125) (Kuwabara et al., 1995).

R-134a, R-143a, and R-236ea have no chlorine atom and thus having a zero ozone depletion potential (ODP) value. R-134a and R-143a are promising alternatives to replace chlorodifluoromethane (R-22) or R-502 (48.8 mass % R-22 + 51.2 mass % R-115) as a component of the binary and/or ternary refrigerant mixtures. And R-236ea is a promising alternative to replace 1,2-dichlorotetrafluoroethane (R-114). This paper reports measurements of the vapor−liquid coexistence curve in the critical region, the determined critical temperature, density, and exponents of the power law, β, and saturation density correlations of R-134a, R-143a, and R-236ea. Previously, we made measurement on R-134a (Kabata et al., 1989), but the sample was of low purity and the results were unreliable, so we measured again concerning R-134a.

Experimental Section

An experimental apparatus used for all measurements has been reported by Okazaki et al. (1983) who originally built it and Tanikawa et al. (1991) who reconstructed it. The details of the apparatus and the procedure have been reported in our previous publications.

The apparatus is composed of three vessels: an optical cell with two synthetic sapphire windows for observing the meniscus of sample refrigerant, a vessel for making expansion, and a vessel for supplying the sample refrigerant. The inner volumes of the optical cell, the expansion vessel, and the supplying vessel are (11.108 ± 0.006) cm^3, (6.297 ± 0.007) cm^3, and (77.457 ± 0.009) cm^3, respectively. These three vessels are assembled on a frame which has a rocking system. This assembly is installed in a thermostated bath containing silicone oil. All measurements were performed by visual observation of the meniscus disappearance in the optical cell.

A 25 Ω standard platinum resistance thermometer placed in the vicinity of the optical cell in the thermostated bath was used for temperature measurements. The temperatures were determined on the 1990 International Temperature Scale (ITS-90) throughout the present paper. In order to keep temperature constant, this platinum resistance thermometer detects the temperature fluctuation and then a PID controller maintains the temperature in the bath.

The experimental uncertainty of the temperature measurement of R-134a and R-143a is estimated to be within ±10 mK as a sum of ±2 mK for the accuracy of the thermometer; ±1 mK for the accuracy of a bridge, and ±7 mK for possible temperature fluctuation in silicone oil in the thermostated bath. For R-236ea, temperature fluctuation is estimated to be ±12 mK because of difficulty in controlling the temperature of the silicone oil at the high temperatures. Therefore the uncertainty of temperature for R-236ea is ±15 mK. The resistance of the platinum resistance thermometer at the triple point of water was calibrated annually. The uncertainty of density measurements is estimated to be between ±0.11%, which is considered due to the uncertainties of the determination of cell volume and sample mass, and ±0.59%, which includes the uncertainty due to expansion procedures.

Purities of samples of R-134a, R-143a, and R-236ea are 99.95%, 99.95 mol %, and 99.9 mol %, respectively. The analysis was performed by the manufacturers, and no further purification was done by ourselves.

Results

The ranges of temperature and density studied and the number of the experimental data points taken for R-134a, R-143a, and R-236ea are summarized in Table 1.

* To whom correspondence should be addressed. TEL.: +81-45-563-1141. FAX.: +81-45-563-5943.

S0021-9568(96)00077-5 CCC: $12.00

Table 1. Ranges of Temperature and Density and the Number of Data Points

	R-134a	R-143a	R-236ea
temp range/K	372.240−T_c	332.658−T_c	408.871−T_c
density range/kg·m^{-3}	367.9−678.0	184.6−729.6	362.4−791.0
no. of vapor data points (ρ'')	9	20	14
no. of liquid data points (ρ')	8	15	13

Table 2. Saturated-Vapor Densities ρ'' of 1,1,1,2-Tetrafluoroethane (R-134a)

T/K	ρ''/kg·m^{-3}	T/K	ρ''/kg·m^{-3}
372.987	367.9 ± 1.6	374.070*	471.5 ± 0.8
373.448	388.9 ± 1.0	374.075*	482.5 ± 1.4
373.784	415.1 ± 0.8	374.075*	505.0 ± 0.6
373.794	416.6 ± 0.8	374.083*	508.4 ± 0.6
374.030*	450.5 ± 1.6		

[a] Asterisk indicates critical opalescence was observed.

Table 3. Saturated-Liquid Densities ρ' of 1,1,1,2-Tetrafluoroethane (R-134a)

T/K	ρ'/kg·m^{-3}	T/K	ρ'/kg·m^{-3}
374.083*	509.5 ± 0.6	373.910	588.9 ± 0.6
374.083*	510.1 ± 0.6	373.880	591.0 ± 1.3
374.079*	513.3 ± 1.1	373.333	633.0 ± 1.0
374.065*	549.8 ± 0.9	372.240	678.0 ± 0.7

[a] Asterisk indicates critical opalescence was observed.

Table 4. Saturated-Vapor Densities ρ'' of 1,1,1-Trifluoroethane (R-143a)

T/K	ρ''/kg·m^{-3}	T/K	ρ''/kg·m^{-3}
355.622	184.6 ± 1.0	345.519	349.4 ± 0.6
337.888	202.5 ± 0.5	345.563	356.8 ± 0.7
339.386	216.8 ± 0.4	345.727*	378.2 ± 0.8
339.837	220.4 ± 0.9	345.821*	399.7 ± 0.8
340.775	232.2 ± 0.3	345.832*	405.1 ± 0.6
342.245	253.9 ± 1.0	345.847*	428.1 ± 0.7
343.206	271.7 ± 0.9	345.847*	432.7 ± 0.5
344.192	289.7 ± 0.8	345.855*	433.3 ± 0.5
344.733	311.0 ± 0.9	345.855*	433.5 ± 0.5
345.280	333.1 ± 0.8	345.856*	433.9 ± 0.5

[a] Asterisk indicates critical opalescence was observed.

Table 5. Saturated-Liquid Densities ρ' of 1,1,1-Trifluoroethane (R-143a)

T/K	ρ'/kg·m^{-3}	T/K	ρ'/kg·m^{-3}
345.861*	434.4 ± 0.5	344.816	555.9 ± 1.0
345.862*	435.4 ± 0.5	344.375	571.1 ± 0.9
345.856*	436.5 ± 0.5	342.379	611.8 ± 0.6
345.864*	436.8 ± 0.5	340.120	655.8 ± 1.0
345.852*	458.5 ± 0.5	338.039	681.3 ± 0.9
345.843*	484.5 ± 1.7	335.933	702.5 ± 0.7
345.616	519.0 ± 1.5	332.658	729.6 ± 0.7
345.295	533.2 ± 1.1		

[a] Asterisk indicates critical opalescence was observed.

The experimental results of each refrigerant including saturated-vapor and saturated-liquid densities are summarized in Tables 2−7. Figures 1−3 show the results on a temperature−density diagram. The measurements when a critical opalescence is observed are given with an asterisk in Tables 2−7 and with solid circles in Figures 1−3.

Concerning R-134a, critical opalescence was observed for nine measurements at densities from (450.5 to 549.8) kg/m^3. For six densities below 471.5 kg/m^3 the meniscus descended with increasing temperature and disappeared at the bottom of the optical cell. For five densities above 549.8 kg/m^3, the meniscus ascended with increasing temperature and disappeared at the top of the optical cell. For the other six densities near the critical density, the meniscus disappeared without reaching either the top or bottom of the optical cell.

Table 6. Saturated-Vapor Densities ρ'' of 1,1,1,2,3,3-Hexafluoropropane (R-236ea)

T/K	ρ''/kg·m^{-3}	T/K	ρ''/kg·m^{-3}
409.875	362.4 ± 1.6	412.365*	529.5 ± 0.8
410.610	383.5 ± 2.3	412.378*	530.9 ± 1.3
411.087	401.4 ± 1.2	412.365*	544.6 ± 1.2
411.680	430.0 ± 1.1	412.376*	564.0 ± 0.6
412.089	460.5 ± 0.9	412.377*	565.0 ± 0.6
412.289*	495.7 ± 1.5	412.370*	567.1 ± 0.6
412.320*	508.4 ± 1.4	412.370*	567.7 ± 0.6

[a] Asterisk indicates critical opalescence was observed.

Table 7. Saturated-Liquid Densities ρ' of 1,1,1,2,3,3-Hexafluoropropane (R-236ea)

T/K	ρ'/kg·m^{-3}	T/K	ρ'/kg·m^{-3}
412.380*	568.2 ± 0.6	411.759	689.4 ± 1.4
412.380*	568.7 ± 1.1	411.640	696.5 ± 0.8
412.370*	583.3 ± 0.9	411.158	720.0 ± 0.8
412.374*	600.9 ± 1.9	410.727	738.4 ± 1.2
412.325*	624.7 ± 0.7	410.032	763.3 ± 0.8
412.238*	643.6 ± 1.7	408.871	791.0 ± 0.8
411.969	672.2 ± 1.1		

[a] Asterisk indicates critical opalescence was observed.

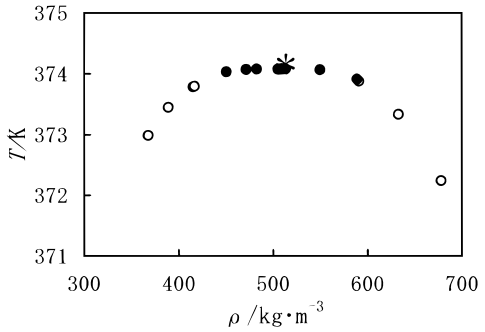

Figure 1. Vapor−liquid coexistence curve of R-134a: (*) critical point; (●, ○) this work.

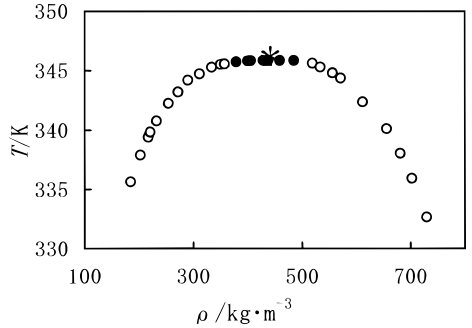

Figure 2. Vapor−liquid coexistence curve of R-143a: (*) critical point; (●, ○) this work.

The critical opalescence was clearly observed in both the liquid and vapor phases, and the meniscus descended slightly before it disappeared when the average density of the sample fluid in the optical cell was 508.4 kg/m^3. Therefore, we found this value should be the saturated-vapor density closest to the critical density among the present measurements in the vapor phase. The opalescence, on the other hand, was observed more intensely in the vapor phase, and the meniscus ascended slightly before it disappeared when the average density was 509.5 kg/m^3, which was the saturated-liquid density value closest to the

Table 8. Comparison of the Critical Temperature and Density for 1,1,1,2-Tetrafluoroethane (R-134a)

author	T_c[a]/K	ρ_c/kg·m^{-3}	purity
Kabata et al. (1989)	374.27 ± 0.01*	508 ± 3	99.8%
Basu and Wilson (1989)	374.23 ± 0.15*	512.2 ± 5	99.95 mass %
Kubota et al. (1989)	374.24 ± 0.05*		99.8 mass %
McLinden et al. (1989)	374.179 ± 0.010*	515.3 ± 1	99.94 mass %
Nishiumi and Yokoyama (1990)	373.02 ± 0.1*		
Fukushima et al. (1990)	374.15 ± 0.03*	507 ± 5	99.99%
Morrison and Ward (1991)	374.255 ± 0.010	515.2 ± 1.5	99.94%
Higashi and Ikeda (1995)	374.11 ± 0.01	511 ± 3	99.98%
Zhelezny et al. (1995)	374.25 ± 0.05	509 ± 3	99.90%
this work	374.083 ± 0.010	509 ± 1	99.95%

[a] A critical temperature value with an asterisk was converted from IPTS-68 to ITS-90.

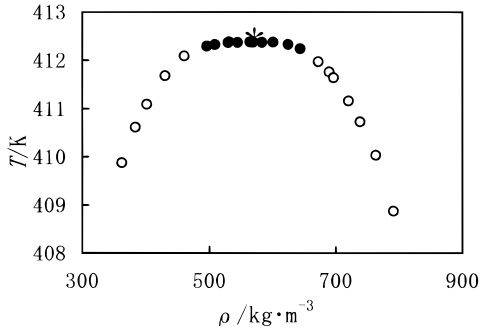

Figure 3. Vapor−liquid coexistence curve of R-236ea: (*) critical point; (●, ○) this work.

critical point among the present measurements in the liquid phase.

Therefore, we surmised that the critical density should be between these two density values. Thus, we determined the critical density for R-134a to be $\rho_c = (509 \pm 1)$ kg/m^3.

The critical temperature can be determined as the saturation temperature which corresponds to the critical density. As shown in Tables 2 and 3, saturation temperature values of three vapor and three liquid densities which are near the critical density, are in good agreement with each other within the experimental uncertainties. Therefore, we determined the critical temperature to be $T_c = (374.083 \pm 0.010)$ K.

For R-143a, critical opalescence was observed for 14 measurements at densities from (378.2 to 484.5) kg/m^3. For 15 densities below 405.1 kg/m^3, the meniscus descended with increasing temperature and disappeared at the bottom of the optical cell. For 9 densities above 519.0 kg/m^3, the meniscus ascended with increasing temperature and disappeared at the top of the optical cell. For the other 11 densities near the critical density, the meniscus disappeared without reaching either the top or bottom of the optical cell.

At a density of 433.9 kg/m^3, the most intense opalescence for R-143a was observed. At this density the meniscus descended slightly before it disappeared. We considered that the density of 433.9 kg/m^3 was slightly lower than the critical density. At 434.4 kg/m^3 the opalescence was also observed quite intensely and the meniscus ascended slightly before it disappeared. We considered that the density of 434.4 kg/m^3 was slightly higher than the critical density. Therefore, the critical density for R-143a should be between these two density values, and we determined the critical density for R-143a to be $\rho_c = (434 \pm 1)$ kg/m^3.

The critical temperature can be determined as the saturation temperature which corresponds to the critical density. As shown in Tables 4 and 5, saturation temperatures of three vapor and five liquid densities which are near the critical density, are in good agreement with each other within the experimental uncertainties. Therefore, we determined the critical temperature to be $T_c = (345.860 \pm 0.010)$ K.

For R-236ea, critical opalescence was observed for 15 measurements at densities from 495.7 to 643.6 kg/m^3. For 9 densities below 530.9 kg/m^3, the meniscus descended with increasing temperature and disappeared at the bottom of the optical cell. For 9 densities above 624.7 kg/m^3, the meniscus ascended with increasing temperature and disappeared at the top of the optical cell. For the other 9 densities near the critical density, the meniscus disappeared without reaching either the top or bottom of the optical cell.

At the density of 567.7 kg/m^3, the most intense opalescence was observed and the meniscus descended slightly before it disappeared. At 568.2 kg/m^3, the opalescence was also observed quite intensely and the meniscus ascended slightly before it disappeared. Therefore, the critical density should be between these two density values, and we determined it to be $\rho_c = (568 \pm 1)$ kg/m^3.

The critical temperature can be determined as the saturation temperature which corresponds to the critical density. As shown in Tables 6 and 7, saturation temperatures of seven vapor and four liquid densities are almost the same within the experimental uncertainties. Therefore, we determined the critical temperature to be $T_c = (412.375 \pm 0.015)$ K.

Discussion

The available information about the critical temperature and density for R-134a is summarized in Table 8. Our T_c value is the lowest among the other T_c values except Nishiumi and Yokoyama (1990), and our ρ_c agrees with those of Kabata et al. (1989), Fukushima et al. (1990), Higashi (1994), and Zhelezny et al. (1995) within their estimated uncertainties. As listed in Tables 2 and 3 we measured saturation densities at six points between (374.075 and 374.083) K near the critical point. We have checked the reproducibility of these values within the experimental uncertainty by six different series of measurement. We believe our results would be the best among the existing measurements.

A similar tabulation is also shown in Table 9 for R-143a. Our T_c value agrees with those reported by Mears et al. (1955), Higashi and Ikeda (1995), and Zhelezny et al. (1995) within the overlapped uncertainties. Our ρ_c values agree well with the data reported by Mears et al. (1955), Fukushima (1993), Higashi and Ikeda (1995), and Zhelezny et al. (1995).

For R-236ea in Table 10, the T_c value reported by Defibaugh and Silva (1994) is higher than our measurement, whereas our ρ_c value is higher than their ρ_c value. Their ρ_c value was determined by extrapolation of the

Table 9. Comparison of the Critical Temperature and Density for 1,1,1-Trifluoroethane (R-143a)

author	T_c[a]/K	ρ_c/kg·m^{-3}	purity
Mears et al. (1955)	346.2 ± 0.5*	434 ± 10	
Arnaud et al. (1991)	346.0 ± 0.1	455 ± 5	99.95%
Fukushima (1993)	345.97 ± 0.03	429 ± 3	99.98 mass %
Higashi and Ikeda (1995)	345.88 ± 0.01	431 ± 3	99.995%
Zhelezny et al. (1995)	345.97 ± 0.36	429 ± 10	99.85%
this work	345.860 ± 0.010	434 ± 1	99.95 mol %

[a] A critical temperature value with an asterisk was converted from IPTS-68 to ITS-90.

Table 10. Comparison of the Critical Temperature and Density for 1,1,1,2,3,3-Hexafluoropropane (R-236ea)

author	T_c/K	ρ_c/kg·m^{-3}	purity
Defibaugh and Silva (1994)	(412.44)	563	99.9 mass %
this work	412.375 ± 0.015	568 ± 1	99.9 mol %

Table 11. Numerical Values of the Coefficients

	D_0	D_1	D_2	B_0	B_1
R-134a	−5.304 46	10.6140	−8.556 22	1.834 78	0.428 076
R-143a	−3.881 13	7.58530	−4.279 78	1.828 58	0.321 215
R-236ea	−19.855 2	33.7792	−2.630 42	1.847 50	0.188 050

rectilinear diameter line to the critical temperature. We believe that the present report is the first direct measurements of the critical parameters of R-236ea.

The critical exponent, β, is used to represent the vapor-liquid coexistence curve in the critical region by means of the following power-law representation;

$$(\rho' - \rho'')/2\rho_c = B[(T_c - T)/T_c]^{\beta} \quad (1)$$

where ρ_c is the critical density, T_c is the critical temperature, single and double primes denote saturated liquid and -vapor phase, respectively, and B is the critical amplitude. Equation 1 requires isothermal pairs of liquid and vapor density values. Hence, we used the following correlation for the calculation of the corresponding saturated-liquid and -vapor densities,

$$(\rho - \rho_c)/\rho_c = D_0\tau^{(1-\alpha)} + D_1\tau + D_2\tau^{(1-\alpha+\Delta_1)} \pm B_0\tau^{\beta} \pm B_1\tau^{(\beta+\Delta_1)} \quad (2)$$

where $\tau = (T_c - T)/T_c$, α and β are critical exponents, and T is the temperature in Kelvin (ITS-90). The exponent Δ_1 stands for the first symmetric correction-to-scaling exponent of the Wegner expansion (Levelt Sengers and Sengers, 1981). From the theoretical background of eq 2, these exponents were determined as follows (Levelt Sengers and Sengers, 1981):

$$\alpha = 0.1085 \qquad \beta = 0.325 \qquad \Delta_1 = 0.50$$

The coefficients D_0, D_1, D_2, B_0, and B_1 in eq 2, were determined by the least-squares fitting to the present measurements and listed in Table 11. In this least-squares fitting, however, we have used seven data out of 17 measured data given in Tables 2 and 3 for R-134a, by excluding five saturated-vapor density and five saturated-liquid density values which all were observed at temperatures higher than T_c/K −0.2. Similarly, we excluded eight saturated-vapor density and six saturated-liquid density values among 35 data points given in Tables 4 and 5 for fitting eq 2 for R-143a, and nine saturated-vapor density and five saturated-liquid density values among 27 data points given in Tables 6 and 7 for fitting eq 2 for R-236ea. The upper sign "+" and the lower "−" of the fourth and fifth terms in eq 2 correspond to the saturated liquid and vapor, respectively. The effective density range of eq 2 is between (367.9 and 678.0) kg/m^3 for R-134a, between (184.6 and 729.6) kg/m^3 for R-143a, and between (362.4 and 791.0) kg/m^3 for R-236ea.

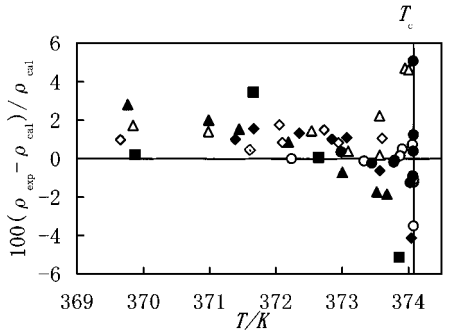

Figure 4. Density deviation of R-134a from eq 2: (○) this work (ρ'); (●) this work (ρ''); (△) Kabata et al. (ρ'); (▲) Kabata et al. (ρ''); (⊡) Basu and Wilson (ρ'); (◇) Fukushima et al. (ρ'); (◆) Fukushima et al. (ρ''); (□) Higashi (ρ'); (■) Higashi (ρ'').

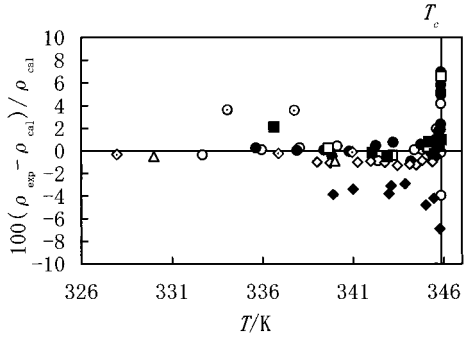

Figure 5. Density deviation of R-143a from eq 2: (○) this work (ρ'); (●) this work (ρ''); (⊙) Mears et al. (ρ'); (⊡) Yokoyama and Takahashi (ρ'); (◇) Fukushima (ρ'); (◆) Fukushima (ρ''); (△) Widiatmo et al. (ρ'); (□) Higashi and Ikeda (ρ'); (■) Higashi and Ikeda (ρ'').

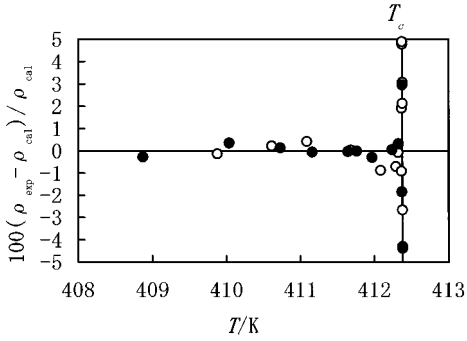

Figure 6. Density deviation of R-236ea from eq 2; (○) this work (ρ'); (●) this work (ρ'').

The density deviations of the present experimental data from eq 2 are shown in Figures 4−6. The standard deviations of input density values from eq 2 are 0.35%, 0.72%, and 0.41% for R-134a, R-143a, and R-236ea, respectively. The deviation plots of R-134a data by Kabata et al. (1989), Basu and Wilson (1989), Fukushima et al. (1990), and Higashi (1994) from eq 2 are shown in Figure 4.

Those of R-143a by Mears et al. (1955), Yokoyama and Takahashi (1991), Fukushima (1993), Higashi and Ikeda (1995), and Widiatmo et al. (1994) are given in Figure 5. Although the difference of density deviation of Fukushima's and Mear's data is found, other measurements are in good agreement with our data. Equation 2 reproduces most of the other measurements within about ±0.5%, respectively.

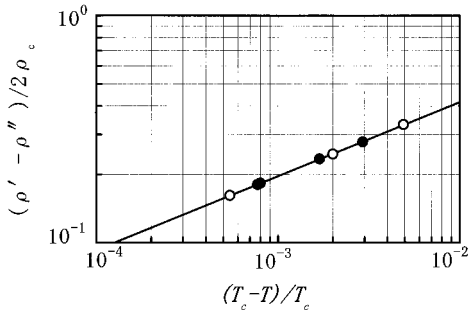

Figure 7. Critical exponent and amplitude of R-134a: (○) this work (ρ'); (●) this work (ρ''); $\beta = 0.3265$; $B = 1.8722$.

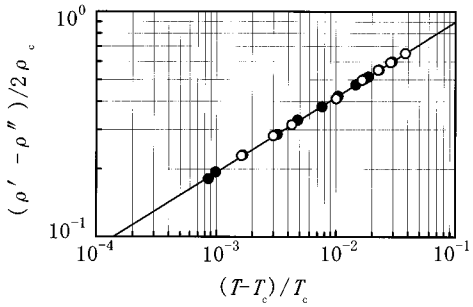

Figure 8. Critical exponent and amplitude of R-143a: (○) this work (ρ'); (●) this work (ρ''); $\beta = 0.3337$; $B = 1.9391$.

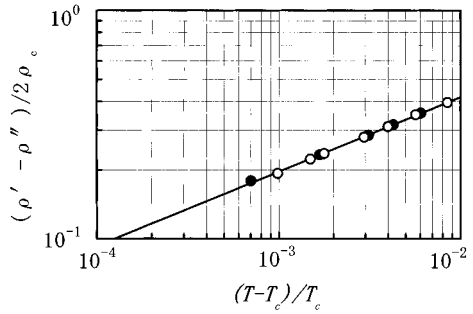

Figure 9. Critical exponent and amplitude of R-236ea: (○) this work (ρ'); (●) this work (ρ''); $\beta = 0.3264$; $B = 1.8759$.

Table 12. Critical Exponent β and the Critical Amplitude B

	β	B
R-134a	0.3265	1.8722
R-143a	0.3337	1.9391
R-236ea	0.3264	1.8759

Figures 7−9 show logarithmic plots in terms of the present measurements and calculated results from eq 2. The power-law representation, eq 1, suggests that the present experimental results can be fitted satisfactorily by a straight line. The slope of the straight line is equivalent to the critical exponent, β. Seven measured data of R-134a, 21 measured data of R-143a, and 13 measured data of R-236ea near the critical point were used for the determination of the critical exponent, β, and the critical amplitude, B, for the least-squares fitting. The β values of R-134a and R-236ea are close to the theoretical value of 0.325 (Levelt Sengers and Sengers, 1981), and the β value of R-143a is greater than the theoretical value as listed in Table 12.

Conclusion

By means of visual observation of the meniscus in the optical cell, 17 saturated-vapor and liquid densities of R-134a, 35 saturated-vapor and -liquid densities of R-143a, and 27 saturated-vapor and -liquid densities of R-236ea in the critical region were measured, and the critical temperatures, the critical densities, and the critical exponents, β, were determined. Saturated-liquid/vapor density correlations for R-134a, R-143a, and R-236ea were developed on the basis of the present measurements.

Acknowledgment

We are indebted to Asahi Glass Co. Ltd., Tokyo, and Daikin Industries Co. Ltd., Osaka, for kindly furnishing the samples. Kunio Mukouyama, who made experiments with the present authors, is gratefully acknowledged.

Literature Cited

Arnaud, D.; Macaudiere, S.; Niveau, L.; Wosinski, S. Thermophysical properties of new refrigerant. The 1,1,1-trifluoroethane (HFC-143a). *Proc. 18th Int. Congr. Refrig.* **1991**, *2*, 664−668.

Basu, R. B.; Wilson, D. P. Thermophysical properties of 1,1,1,2-tetrafluoroethane(R-134a). *Int. J. Themophys.* **1989**, *10*, 591−603.

Defibaugh, D. R.; Silva, A. M. Compress liquid densities, saturated liquid densities and vapor pressure of 1,1,1,2,3,3-hexafluoropropane (HFC-236ea). Paper presented at the 12th Symposium on Thermophysical Properties, 1994.

Fukushima, M. Measurement of vapor pressure, vapor liquid coexistence curve and critical parameters of HFC-143a. (In Japanese) *Trans. JAR* **1993**, *10*, 87−93.

Fukushima, M.; Watanabe, N.; Kamimura, T. Measurements of the vapor-liquid coexistence curve and the critical parameters of HCFC-123 and HFC-134a. *Trans. JAR* **1990**, *7*, 85−95.

Higashi, Y. Critical parameters for HCFC134a, HCFC32 and HFC125. *Int. J. Refrig.* **1994**, *17*, 524−531.

Higashi, Y.; Ikeda, T. Critical parameters for 1,1,1-trifluoroethane (R-143a). *Proc. 4th Asian Thermophys. Prop. Conf.* **1995**, *2*, 279−282.

Higashi, Y.; Okazaki, S.; Takaishi, Y.; Uematsu, M.; Watanabe, K. Measurements of the vapor−liquid coexistence curve for the binary R12+R22 system in the critical region. *J. Chem. Eng. Data* **1984**, *29*, 31−36.

Higashi, Y.; Uematsu, M.; Watanabe, K. Measurements of the vapor−liquid coexistence curve and determination of the critical parameters for refrigerant 13B1. *Trans. JSME* **1985**, *28*, 2660−2666.

Higashi, Y.; Ashizawa, M.; Kabata, Y.; Majima, T.; Uematsu, M.; Watanabe, K. Measurements of vapor pressure, vapor−liquid coexistence curve and critical parameters of refrigerant 152a. *JSME Int. J.* **1987**, *30*, 1106−1112.

Kabata, Y.; Tanikawa, S.; Uematsu, M.; Watanabe, K. Measurements of the vapor-liquid coexistence. *Int. J. Themophys.* **1989**, *10*, 605−616.

Kubota, H.; Yamashita, T.; Tanaka, Y.; Makita, T. Vapor pressures of new fluorocarbons. *Int. J. Themophys.* **1989**, *10*, 629−638.

Kuwabara, S.; Aoyama, H.; Sato, H.; Watanabe, K. Vapor-liquid coexistence curve in the critical region and the critical temperatures and densities of difluoromethane and pentafluoroethane. *J. Chem. Eng. Data* **1995**, *40*, 112−116.

Levelt Sengers, J. M. H.; Sengers, J. V. In *Perspectives in Statistical Physics*; Raveche, H. J., Ed.; North-Holland: Amsterdam, 1981; Chapter 14.

McLinden, M. O.; Gallagher, J. S.; Weber, L. A.; Morrison, G.; Ward, D. K.; Goodwin, A. R. H.; Moldover, M. R.; Schmidt, J. W.; Chae, H. B.; Bruno, T. J.; Ely, J. F.; Huber, M. L. Measurement and formulation of the thermodynamic properties of refrigerants 134a(1,1,1,2-tetrafluoroethane) and 123(1,1-dichloro-2,2,2-trifluoroethane). *ASHRAE Trans.* **1989**, *95*, 263−283.

Mears, W. H.; Stahl, R. F.; Orfeo, R. C.; Kells, L. F.; Thompson, W.; McCan, H. Thermodynamic properties of halogenated ethanes and ethylenes. *Ind. Eng. Chem.* **1955**, *47*, 1449−1454.

Morrison, G.; Ward, D. K. Thermodynamic properties of two alternative refrigerants: 1,1-dichloro-2,2,2-trifloroethane(R123) and 1,1,1,2-tetrafluoroethane(R134a). *Fluid Phase Equilib.* **1991**, *62*, 65−86.

Nishiumi, H.; Yokoyama, T. Vapor-liquid equilibrium for the system of R134a-R22. *Proc. 11th Japan Symp. Thermophys. Prop.* **1990**, 95−98.

Okazaki, S.; Higashi, Y.; Takaishi, Y.; Uematsu, M. Watanabe, K. Procedures for determining the critical parameters of fluids. *Rev. Sci. Instrum.* **1983**, *54*, 21−25.

Tanikawa, S.; Kabata, Y.; Sato, H.; Watanabe, K. Measurements of the critical parameters and the vapor-liquid coexistence curve in the critical region of HCFC-123. *J. Chem. Eng. Data* **1991**, *35*, 381−385.

Tanikawa, S.; Tatoh, J.; Maezawa, Y.; Sato, H.; Watanabe, K. Vapor-liquid coexistence curve and the critical parameters of 1-chloro-1,1-difluoroethane(HCFC-142b). *J. Chem. Eng. Data* **1992**, *37*, 74−76.

Tatoh, J.; Kuwabara, S.; Sato, H.; Watanabe, K. Measurements of the vapor-liquid coexistence curve in the critical region and the critical parameters of 1,1,2,2-tetrafluoroethane. *J. Chem. Eng. Data* **1993**, *38*, 116−118.

Weber, L. A.; Levelt Sengers, J. M. H. Critical parameters and saturation densities of 1,1-dichloro-2,2,2-trifluoroethane. *Fluid Phase Equilib.* **1990**, *55*, 241−249.

Widiatmo, J. V.; Sato, H.; Watanabe, K. Saturated-liquid densities and vapor pressures of 1,1,1-trifluoroethane, difluoromethane, and pentafluoroetane. *J. Chem. Eng. Data* **1994**, *39*, 304−308.

Yokoyama, C.; Takahashi, S. Saturated liquid densities of 2,2-dichloro-1,1,1-trifluoroethane (HCFC-123), 1,2-dichloro-1,2,2-trifluoroethane (HCFC-123a), 1,1,1,2-tetrafluoroethane(HFC-134a). *Fluid Phase Equilib.* **1991**, *67*, 227−240.

Zhelezny, V.; Chernyak, Y.; Zhelezny, P. Critical parameters for the several alternative mixtures. *Proc. 4th Asian Thermophys. Prop. Conf.* **1995**, *2*, 291−294.

Received for review February 23, 1996. Accepted May 14, 1996.[⊗]

JE960077W

[⊗] Abstract published in *Advance ACS Abstracts,* July 1, 1996.